Power Performance of X-band Si/$Si_{0.75}Ge_{0.25}$/Si HBTs

Zhenqiang Ma, Saeed Mohammadi, Pallab Bhattacharya, Linda P. B. Katehi
Department of Electrical Engineering and Computer Science
University of Michigan, Ann Arbor, MI 48109-2122

Samuel A. Alterovitz, and George E. Ponchak,
NASA Glenn Research Center
21000 Brookpark Road, Cleveland, OH 44135

***Abstract*---High performance power SiGe/Si HBTs at X-band (8.4 GHz) frequency have been demonstrated. Under continuous wave operation, a single 10-finger Si/$Si_{0.75}Ge_{0.25}$/Si (emitter area of 780 μm^2) HBT, biased at class AB, exhibits 29% peak PAE operating in common-emitter (C-E) mode and 42.1% peak PAE in common-base (C-B) mode with 25.7 dBm and 25 dBm P_{out} at peak PAE, respectively. The power gain at peak PAE for C-E and C-B mode operation is 6.1 dB and 7.1 dB, respectively. A 20-finger C-B HBT is capable of delivering 28.45 dBm (700 mW) of RF output power with 25% associated PAE. The peak PAE achieved with 20-finger C-B HBT is 32% with concurrent output power of 27.4 dBm. These represent the state-of-the-art power performance of SiGe-based HBTs. The performance difference between the common-emitter mode and the common-base mode has been analyzed.**

1. INTRODUCTION

SiGe-based HBTs have undergone substantial investigations over the past decades. High-speed operation of these devices has been proved to be readily feasible with both f_{max} and f_T over 100 GHz [1]-[3]. With these performances, they are also suitable for Si-based microwave and millimeter wave applications. Particularly, the fact, that SiGe-based material system is compatible with CMOS technology, provides the opportunity to integrate RF/microwave modules with low-frequency CMOS circuitry and hence offers the feasibility of realizing a complete wireless system on a chip. On the other hand, it has long been a concern to realize efficient power amplifiers with SiGe material system. Bipolar junction transistors (BJTs) are more suitable for power applications than field effect transistors (FETs) in terms of linearity, higher voltage operation, power-handling capability and etc. However, the investigations on the microwave power application of SiGe-based HBTs have so far been limited only up to C-band [4]-[11] frequencies. Higher frequency operation (X-band and beyond) is readily desired for higher channel capacity in wireless communication and only very limited performance characteristics of SiGe HBTs [12] [13] in X-band have been reported. The obstacle in developing high-performance X-band power SiGe HBTs arises from: (a) in order to obtain high output power from the device, high breakdown voltages and large area are usually needed. Associated with the high breakdown voltages and large device area is poor frequency response and, hence, at a certain operating frequency a low power gain is resulted. In this case without sacrificing linearity high efficiency power amplifiers cannot be realized. In addition, thermal effects are servere for large-area devices and the power gain is further reduced; (b) the intrinsic -6dB/octave power gain reduction of a certain device will lead to a lower power gain when operating the device at higher frequencies than lower frequencies; (c) large-signal operation result in gain compression and a high power gain at high input power level is not easily achieved. Practically, a high output power with a concurrent high power gain (hence PAE at a certain class of operation) is always required for the implementation of efficient power amplifiers. In this paper, we report the state-of-the-art large-signal performance of Si/SiGe/Si power HBTs, fabricated from heterostructures grown by one-step chemical vapor deposition (CVD).

2. DEVICE DESIGN AND FABRICATION

High power operation of SiGe HBTs requires high device breakdown voltages. The design of a Si/SiGe/Si power HBT includes vertical heterostructure design ---- focusing on the determination of thickness, composition and doping

0-7803-7129-1/01/$10.00 (C) 2001 IEEE

concentration of each layer, and lateral layout design, which relates to the device active area, suppression of heat dissipation and performance optimization. The design goal for a power HBT is to achieve high-frequency operation while maintaining high breakdown voltages and high current level for high output power. Regardless of the fact that the design of base and emitter regions influences the HBT performance [14], the design of the collector region has a more profound effect on the overall performance of a power HBT [15]. Device performance characteristics such as collector-base avalanche breakdown voltage (BV_{CBO}), maximum collector current density ($J_{C,\,max}$), carrier total transit delay time from emitter to collector (τ_{EC}) and base-collector junction capacitance (C_{BC}) are mainly determined by collector thickness and doping concentration. A detailed discussion on the heterostructure design can be found in our previous publication [16]. In this study, a collector doping concentration of $3x10^{16}cm^{-3}$ is chosen with the objective of having a large breakdown voltage for a collector thickness of 500 nm. The heterostructure, which is grown on high-resistivity 4" Si wafer in one step by CVD, is shown in Fig. 1. The measured SIMS profile of the device is shown in Fig. 2. The maximum boron concentration of $8x10^{19}$ cm^{-3} ensures a low base access/spreading resistance of the $Si_{0.75}Ge_{0.25}$ layer. The thickness of the sub-collector layer is chosen to be 1μm, to achieve a smaller collector access/spreading resistance. The doping concentration in both the emitter cap layer and the sub-collector layer is ~$2x10^{19}$ cm^{-3}, which is the upper limit that can be achieved with in-situ doping during CVD growth.

The layout design consideration is also detailed in Ref. 16 and the description of the double-mesa type SiGe/Si HBTs fabrication process can be found in Ref. 17. Figure 3 shows the micrograph of a finished 10-finger common-base HBT with the total emitter area of 780 μm^2.

3. DEVICE PERFORMANCE

A. DC and small-signal RF performance

The DC characteristics of the fabricated 10-finger (emitter area is 780 μm^2) common-emitter (C-E) and common-base (C-B) SiGe/Si HBTs were characterized with an HP 4145B semiconductor parameter analyzer. The measured base-collector

Emitter cap	Si	n+	P	$2x10^{19}$ cm^{-3}	150 nm
Emitter	Si	n	P	$1x10^{18}$ cm^{-3}	100 nm
Spacer	$Si_{0.75}Ge_{0.25}$	i			5 nm
Base	$Si_{0.75}Ge_{0.25}$	p+	B	$1x10^{20}$ cm^{-3}	20 nm
Spacer	$Si_{0.75}Ge_{0.25}$	i			5 nm
Collector	Si	n-	P	$3x10^{16}$ cm^{-3}	500 nm
Sub-collector	Si	n+	P	$2x10^{19}$ cm^{-3}	1000 nm
Substrate	Si(100)	p-		$1x10^{12}$ cm^{-3}	540 μm

Figure 1: Epitaxial structure of the X-band power SiGe/Si HBTs. All the values are designed values.

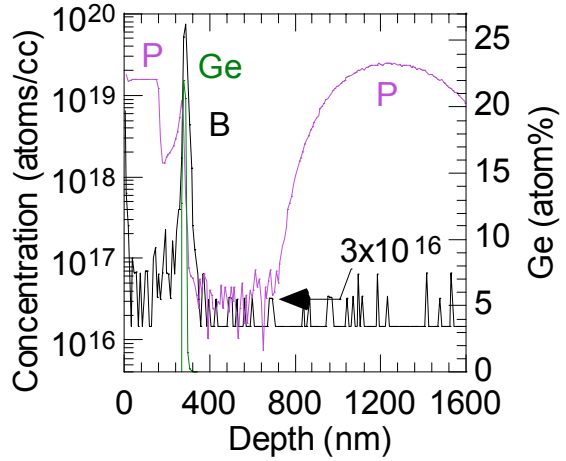

(a)

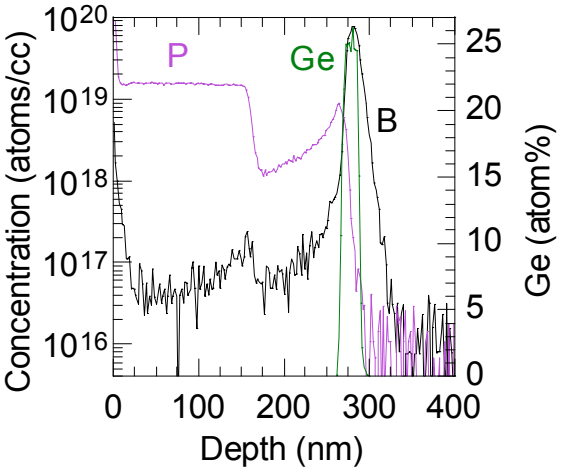

(b)

Figure 2: Measured SIMS profiles of the CVD grown X-band power SiGe/Si HBTs : (a) showing the complete structure; (b) with a detailed analysis of the emitter and base layers.

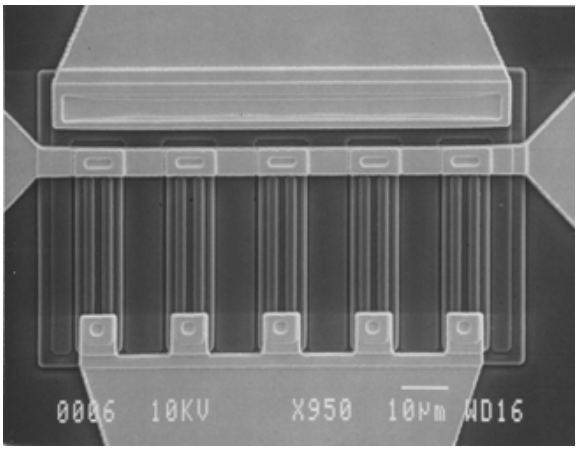

Figure 3: Photomicrograph of the fabricated 10-finger C-B SiGe/Si power HBT.

breakdown voltage (BV_{CBO}) is about 26 V and the open-base collector-emitter breakdown voltage (BV_{CEO}) is about 23 V. No punchthrough was observed at these voltages. The high breakdown voltages result from the low collector doping concentration and the high base doping concentration (Fig. 2), which allow high-applied operation voltages for power amplification and can accommodate large output signal swing. High power can then be obtained with large device area. Another advantage of these high breakdown voltages is better linearity of output power. The common-emitter current gain β was measured to be in the range of 25-30 and the highest differential current gain $\Delta\beta$ was measured to be 38.3.

The small-signal RF performance characteristics of the 10-figner SiGe/Si HBTs were characterized by small-signal S-parameters with an HP 8510C network analyzer. Figure 4 shows the RF response of 10-finger C-E and C-B HBTs under the optimum bias conditions. The C-E HBT demonstrates f_T of 29.5 GHz and f_{max} of 40 GHz based on –6dB/octave roll-off (Fig. 4(a)). Beyond 24 GHz, a –12dB/octave roll-off is observed, which is due to the 2nd pole generated by large base-collector junction capacitance C_{BC}. The large size of base-emitter junction area is relative to the emitter area (intrinsic base-collector junction area). The base-collector junction area A_{BC} for a 10-finger HBT with a distributed layout is larger than that for a compact layout (all 10 fingers bound togerher) with the same number of emitter fingers. The ratio between the intrinsic base-collector junction area and the total junction area A_{BC} is about 0.35 for the distributed layout and that for a 10-finger compact layout is about 0.45. The MSG/MAG curve beyond 9 GHz does not strictly follow the roll-off of –6dB/octave, which is also because of the 2nd pole generation. The power gain at 8.4 GHz is MSG = 12.4 dB and U = 13.0 dB. It is noteworthy that the unilateral gain U is larger than MSG/MAG for the C-E HBT. In C-E configuration, the input port is base and the output port is collector. The feedback path from the output port (collector) to the input port (base) is the base-collector junction capacitance, C_{BC}. Because of the large value of C_{BC}, the power gain represented by U is "exaggerated" relative to that represented by MSG/MAG.

The C-B HBT demonstrates a higher f_{max} of 74 GHz based on the extrapolation of –6dB/octave roll-off (Fig. 4(b)), which is much larger than that of C-E HBT with the same active area layout. Due to the 2nd pole generated by junction capacitance, the MSG/MAG curve beyond 31 GHz follows a gain roll-off of –12dB/octave. The MSG below 5 GHz does not follow –3dB/octave roll-off, which is influenced by the 1st pole. The power gain at 8.4 GHz is MAG = 18.9 dB and U = 14.1 dB. The MAG value at 8.4 GHz of C-B HBT is much larger than that of C-E HBT, indicating a much better power performance for C-B HBT than C-E HBT. Contrary to the RF response of C-E HBT, the MSG/MAG values are larger than the values of U for almost all the measured frequency range as seen in Fig. 4(b). The reason which causes a difference in the RF characteristics between C-E and C-B HBTs is now analyzed.

In a common-emitter HBT, the feedback path between the output port (collector) and the input port (base) is C_{BC}. In C-B HBT, the input port is the emitter and the ouput port is the collector. The feedback path from the output port to the input port is C_{EC}, which is a series capacitance with C_{BE} and C_{BC}. Since C_{EC} is always smaller than C_{BC}, the feedback from the output port (collector) to the input port (emitter) for the C-B HBT is smaller than that of the C-E HBT. As a result, the MSG/MAG of the C-B HBT is larger than that of the C-E HBT. In terms of the power gain, C-B HBT is more appropriate for the application of power amplification than C-E HBT. Since a C-B HBT does not have current gain, the current gain shown in Fig. 4(b) is less than 0 dB at low frequencies. The current gain peak at high frequencies is due to the resonance caused by the parasitic inductance of the output port and C_{BC}. The parasitic inductance

mainly arises from the interdigitated collector metal of the distributed layout. This phenomenon has been described in our previous publication [13].

To determine the amplification characteristics of the 10-finger C-B HBT, the collector dependence of f_{max} was measured. The results are shown in Fig. 5. Due to the influence of the 1st pole and the 2nd pole, the power gain curves do not strictly follow the –6dB/octave roll-off. The values of f_{max} shown in Fig. 5 were calculated from the power gain value (MAG) at 10 GHz based on –6dB/octave roll-off. It is obvious that there is a large collector current range in which the C-B HBT shows the optimum RF response. The roll-off of f_{max}, which is due to the Kirk effect, was not measured for the concern of the device burn-out.

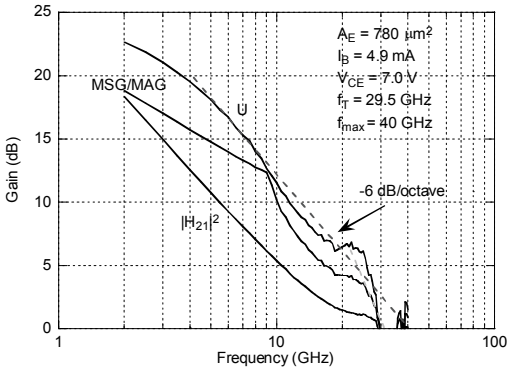

(a)

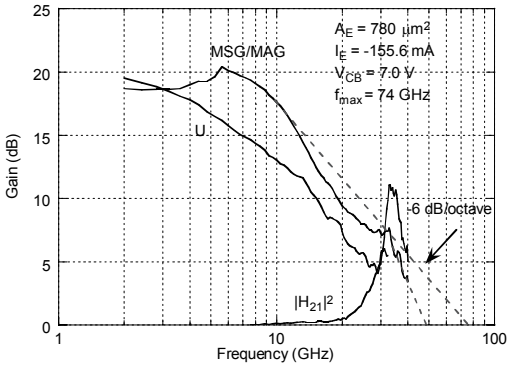

(b)

Figure 4: Frequency response of 10-finger (A_E = 780 μm²) SiGe/Si HBTs showing current gain and power gain. f_T and f_{max} are extrapolated based on the assumption of –6dB/octave roll-off: (a) C-E HBT; (b) C-B HBT.

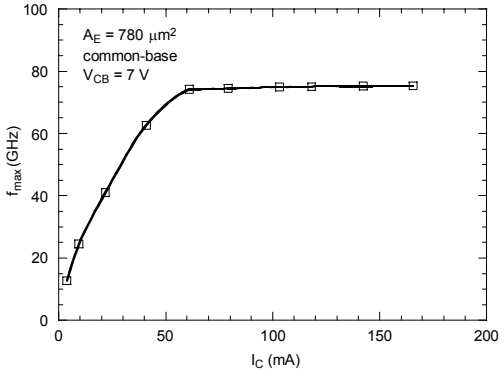

Figure 5: f_{max} versus collector current I_C for 10-finger (A_E = 780 μm²) SiGe/Si HBTs fabricated from structure HBT_2.

B. Large-signal RF characteristics

The 10-finger C-E and C-B SiGe/Si HBTs were characterized with a Focus Microwave source/load pull system. The output power P_{out}, power gain and the power added efficiency PAE ($PAE = \frac{P_{out} - P_{in}}{P_{DC}}$) were measured on wafer as a function of input power P_{in} at 8.4 GHz under CW mode. No special heat dissipation technique or external ballast resistors were involved in the measurements. Figure 6 shows the power performance of 10-finger C-E and C-B HBTs along with the collector current under different bias conditions. When the C-E HBT was biased at V_{CE} = 7 V and V_{BE} = 1.14 V (class A), the linear gain of 8.88 dB was obtained. The matching points (Γ_S = $0.82\angle 178^o$ and Γ_L = $0.57\angle 142^o$) were optimized for maximum P_{out}. The input matching is very close to the edge of the Smith chart, indicating the small input impedance. The output power at 1 dB gain compression point, $P_{out, -1dB}$ is 22.8 dBm. The peak PAE of 28.2% was achieved at 3.5 dB gain compression point with a P_{out} of 25.9 dBm. At the quiescent bias point, the collector current is 62 mA and it was driven to 147 mA at the peak PAE. The power gain at the peak PAE was measured to be 5.4 dB. The final saturation power was not measured owing to the DC current limit, which was set to prevent the device from burning out. No oscillation was observed during measurement. Slightly higher peak PAE (29%) was obtained with the same input and output matching when V_{BE} was lowered to 1.07 V. The P_{out} at the peak PAE is 25.7 dBm, which was obtained at 2.8 dB gain compression. The collector current at the quiescent point is about 45 mA, which

is close to a class AB operation. Owing to the lower V_{BE}, a lower linear gain 8.06 dB was resulted. The above performance features represent the typical behavior of SiGe/Si power HBTs, which can be summarized as the following. High bias levels (fixed V_{CE} and variable V_{BE}) provide higher linear gain than low bias levels, but with an earlier gain compression as input power is increased. However, higher PAE can be obtained at the low bias levels than the high bias levels. The causes for these features are analyzed.

At the high bias levels (class A or higher), the collector current at the quiescent point is close to the upper limit of the collector current $I_{C,max}$, which is set by the decrease in the value of β (Kirk effect). As P_{in} is driven to higher levels the swing of the output signal will be quickly limited by the maximum collector current, $I_{C,max}$. A direct consequence of the high bias levels is an early power gain compression and large output distortion (not measured in this work) with the increasing of the input power. Usually, the high bias levels are used for small-signal (output signal swing is not limited by $I_{C,max}$) and high gain operation. As the bias level is lowered, the output signal swing will be less limited by the collector current and the output power can be driven into higher level with the increasing of the input power. Therefore, slower power gain compression with input power can be resulted. The high PAE which can be realized at the low bias levels is due to the low DC power dissipation (low I_C and/or smaller conduction angle) while the output signal can reach a large and undistorted swing. The lower linear gain at the low bias levels is mainly due to the fact that a smaller collector current will result in a lower f_T and thus f_{max}. Since at the low bias levels the peak PAE can be reached at a lower P_{in} level, the P_{out} at the peak PAE under the low bias levels is smaller than that under the high bias levels.

The 10-finger C-B HBT shows better performance than C-E HBT with the same bias-dependent features. Under V_{CB} = 7 V and V_{EB} = -1.21 V (class AB), the quiescent collector current is 49.4 mA. With the input/output matching ($\Gamma_S = 0.82\angle 178^o$ and $\Gamma_L = 0.67\angle 112^o$) optimized for maximum output power, 25 dBm was obtained at the peak PAE of 40.4%. Higher P_{out} at the peak PAE can be obtained if the bias levels were set higher. A linear gain of 12 dB was measured and the peak PAE was achieved at 3.4 dB power gain compression. The associated power gain at the peak

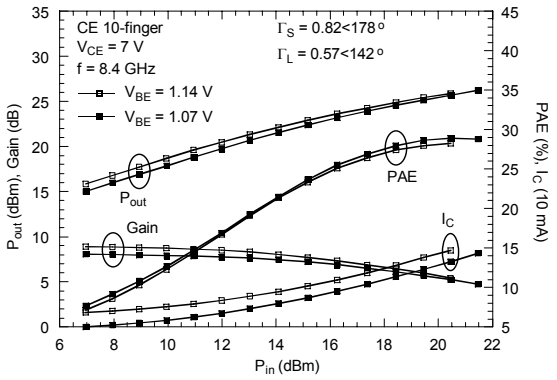

(a)

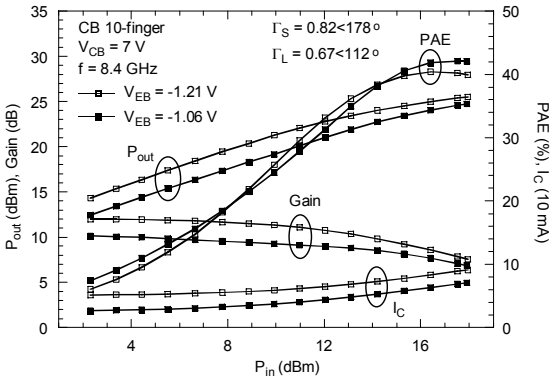

(b)

Figure 6: Meaured P_{out}, Gain, PAE and I_C of 10-finger (a) C-E and (b) C-B SiGe/Si HBTs fabricated from structure HBT_2.

PAE is 8.6 dB. The high power gain associated with C-B HBT is mainly ascribed to a small C_{EC}. After V_{EB} is lowered to –1.06 V, with the same matching a peak PAE of 42.1% was achieved. The P_{out} at the peak PAE is 24.6 dBm with the associated power gain of 7.1 dB (3.07 dB gain compression). A more slowly compressed power gain was measured for V_{EB} = –1.06 V than for V_{EB} = -1.21 V. It is interesting to note that the best input matching point for C-E HBT and that for C-B HBT are the same with different output matching points. This is because no matter for C-E or C-B configuration, the input port and the ground are always base and emitter, which is not the case for the output port and ground.

The power performance of 20-finger C-E and C-B HBTs with an identical layout, were also characterized on wafer under CW mode at 8.4 GHz. The input and output matching ($\Gamma_S = 0.82\angle 180^o$ and $\Gamma_L = 0.71\angle 154^o$) was optimized for the maximum P_{out}. The P_{out}, Gain, PAE along with the collector current I_C as a function of P_{in} are illustrated in Fig. 7.

For the C-E 20-finger HBT, under V_{CE} = 7 V and V_{BE} = 1.08 V (close class AB), 27.4 dBm P_{out} was obtained at the peak PAE of 26.3%. The linear power gain is 5.5 dB and it was compressed to 4 dB at the peak PAE. Higher PAE can be achieved with lower bias levels. Again, much better power performance was obtained from the 20-finger C-B HBTs. With the optimum input and output matching ($\Gamma_S = 0.82\angle 180^o$ and $\Gamma_L = 0.83\angle 150^o$) and under V_{CE} = 7 V and V_{BE} = 1.48 V (class A), P_{out} of 27.4 dBm ($P_{out,RF}$ = 550 mW) was realized at the peak PAE of 32% with the associated power gain of 7 dB. At the peak PAE, the initial linear power gain 10.9 dB was compressed by 3.9 dB. After the fall-off of the peak PAE to 25%, a P_{out} of 28.45 dBm (700 mW) was reached. To the authors' best knowledge, these are the best RF power performance achieved with SiGe/Si HBTs at X-band, till date. With the consideration of the emitter undercut during KOH wet etching (actual emitter area is about

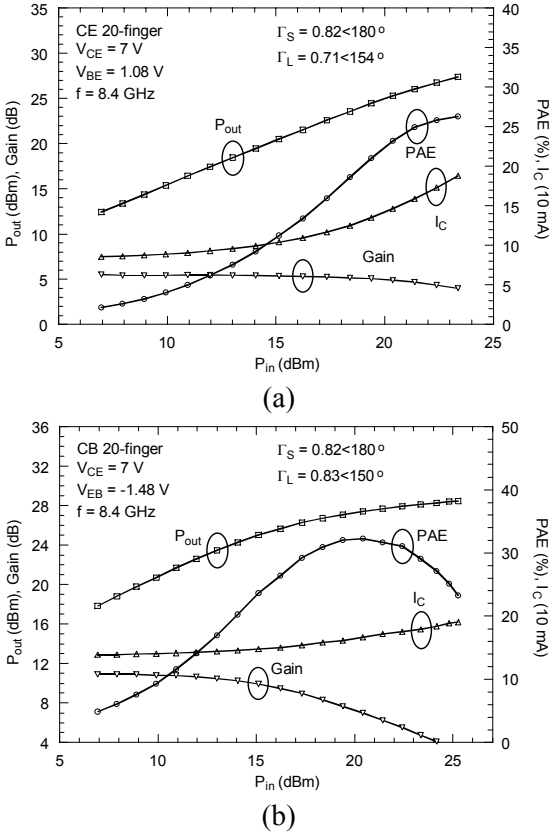

Figure 7: Meaured P_{out}, Gain, PAE and I_C of 20-finger (a) C-E and (b) C-B SiGe/Si HBTs fabricated from structure HBT_2.

1200 μm^2), the power density in this device is 0.58 mW/μm^2. Higher RF power density (0.96 mW/μm^2) has been achieved from a smaller C-E HBT (4-finger with the same type of layout) fabricated from the same wafer. These parameters (for both 4-figner C-E, 10- and 20-finger C-E and C-B HBTs) represent the state-of-the-art power performance of SiGe-based HBTs operating at X-band frequencies at the present time. A lower RF power density for larger devices is resulted from the thermal effect such that the power gain is reduced. The employment of a distributed layout and a low-level collector doping concentration in this study helps to reduce the thermal effects to a minimum level. Better power performance was not obtained from 30-finger HBTs, mainly because of the severe thermal effects and the difficulty of output matching.

4. CONCLUSION

In this paper, the DC, small- and large-signal RF characteristics of Si/$Si_{0.75}Ge_{0.25}$/Si power HBTs have been described and analyzed. An optimized heterostructure design and distributed layout lead to the state-of-the-art power HBT performance characteristics. High breakdown voltages have been realized in large emitter area (780 μm^2) SiGe-based HBTs, with 23 V BV_{CEO} and 26 V BV_{CBO} and associated 40 GHz and 74 GHz of f_{max} for C-E and C-B HBTs, respectively. 25.7 dBm P_{out} was obtained from 10-finger C-E HBTs at a peak PAE of 29%. The associated power gain at the peak PAE is 6.1 dB. 10-finger C-B HBTs provide 25 dBm P_{out} at a peak PAE of 40.4% with associated power gain of 8.6 dB. A higher PAE of 42.1% was achieved at slightly lower bias levels. 20-finger SiGe/Si HBTs demonstrated the highest P_{out} at thepeak PAE, 27.4 dBm (550 mW) for both C-E and C-B configurations. Peak PAE of 26.3% and 32% were measured for 20-finger C-E and C-B HBTs, respectively. The associated power gain at the peak PAE for C-E and C-B HBTs are 4 dB and 7 dB, respectively. With 25% PAE, 20-finger HBTs are able to provide 28.45 dBm (700 mW) P_{out}, which is equivalent to a RF power density of 0.58 mW/μm^2. The highest power density was measured to be 0.96 mW/μm^2 from 4-finger C-E HBTs. These superior SiGe/Si HBT power performance results from a very low base resistance, high device breakdown voltages and good thermal stability of the device at very high power levels, which are further ascribed to a combination of device heterostructure design and

optimized layout, good material quality and optimized processing techniques.

Acknowledgement

This work is being supported by NASA/JPL under contract 1218483 and NASA-GRC under Grant NCC3-790.

REFERENCES

[1] A. Schüppen, U. Erben, A. Gruhle, H. Kibbel, H. Schumacher, and U. König, "Enhanced SiGe heterojunction bipolar transistors with 160 GHz-f_{max}," in *IEDM Tech. Dig.*, Washington, DC, Dec. 1995, pp. 743-746.

[2] E. F. Crabbé, B. S. Meyerson, J. M. C. Stork, and D. L. Harame, "Vertical profile optimization of very high frequency epitaxial Si- and SiGe-base bipolar transistors," in *IEDM Tech. Dig.*, Washington, DC, Dec. 1993, pp. 83-86.

[3] K. Oda, E. Ohue, M. Tanabe, H. Shimamoto, T. Onai, and K. Washio, "130 GHz-f_T SiGe HBT technology," in *IEDM Tech. Dig.*, Washington, DC, Dec. 1997, pp. 791-794.

[4] A. Schüppen, S. Gerlach, H. Dietrich, D. Wandrei, U. Seiler, and U. König, "1-W SiGe power HBT's for mobile communication," *IEEE Microwave Guided Wave Lett.*, vol. 6, pp. 341-343, Sept. 1996.

[5] D. R. Greenberg, M. Rivier, P. Girard, E. Bergeault, J. Moniz, D. Ahlgren, G. Freeman, S. Subbanna, S. J. Jeng, K. Stein, D. Nguyen-Ngoc, K. Schonenberg, J. Malinowski, D. Colavito, D. L. Harame, and B. Meyerson, "Large-signal performance of high-BV_{CEO} graded epi-base SiGe HBTs at wireless frequencies," in *IEDM Tech. Dig.*, Washington, DC, Dec. 1997, pp. 799-802.

[6] G. N. Henderson, M. F. O'Keefe, T. E. Boles, P. Noonan, J. M. Sledziewski, and B. M. Brown, "SiGe bipolar junction transistors for microwave power applications," in *IEEE MTT-S Symp. Dig.*, Denver, CO, June 1997, pp. 1299-1302.

[7] R. Götzfried, F. Beiβwanger, S. Gerlach, A. Schüppen, H. Dietrich, U. Seiler, K.-H. Bach and J. Albers, "RFIC'c for mobile communication systems using SiGe bipolar technology," *IEEE Trans. Microwave Theory Tech.*,. vol. 46, pp. 661-668, May 1998.

[8] A. Schüppen, "SiGe-HBTs for mobile communication," *Solid State Electro.*, vol. 43, pp. 1373-1381, Aug.1999.

[9] P. A. Potyraj, K. J. Petrosky, K. D. Hobart, F. J. Kub and P. E. Thompson, "A 230-W S-band SiGe heterojunction bipolar transistor," *IEEE Trans. Microwave Theory Tech.*,. vol. 44, pp. 2392-2397, Dec. 1996.

[10] J. N. Burghartz, J.-O. Plouchart, K. A. Jenkins, C. S. Webster and M. Soyuer, "SiGe power HBT's for low-voltage, high-performance RF applications," *IEEE Electron Device Lett.*, vol. 19, pp. 103-105, April, 1998.

[11] U. Erben, M. Wahl, A. Schüppen, and H. Schumacher, "Class-A SiGe HBT power amplifiers at C-band frequencies," *IEEE Microwave Guided Wave Lett.*, vol. 5, pp. 435-436, Dec. 1995.

[12] R. Strong, A. Agarwal, T. Smith, R. Messham, S. Mani, V. Hegde, M. Hanes, H. Nathanson, P. Potyraj, K. Petrosky, T. Knight and P. Brabant, "X-band SiGe power HBT's," in *1998 Topical Meeting on Silicon Monolithic Integrated Circuits in RF Systems. Digest of Papers*, Ann Arbor, MI, Sept. 1998, pp.57-60.

[13] J.-S. Rieh, L.-H. Lu, Z. Ma, X. Liu, L. P. B. Katehi and P. Bhattacharya and E. T. Croke, "Small- and large-signal operation of X-band CE and C-B SiGe/Si power HBTs," in *IEEE MTT-S Symp. Dig.*, Anaheim, CA, June 1999, pp. 1191-1194.

[14] A. Gruhle, "SiGe heterojunction bipolar transistors," in *Silicon-based millimeter-wave devices*, Ed. J.-F. Luy and P. Russer, Springer Series in Electronics and Photonics, vol. 32, Springer-Verlag, Berlin, Germany, 1994, , pp.149-192.

[15] M. E. Kim, B. Bayraktaroglu and A. Gupta, "HBT devices and circuit applications," in *HEMTs and HBTs: devices, fabrication and circuits*, Ed. F. Ali and A. Gupta, Artech House, Norwood MA, 1991.

[16] Z. Ma, S. Mohammadi, P. Bhattacharya, L.P. B. Katehi, S. A. Alterovitz, and G. E. Ponchak, "A high power and high gain X-band Si/SiGe/Si heterojunction bipolar transistor," accepted for publication in *IEEE Trans. Microwave Theory and Tech.*, 2001.

[17] J.-S. Rieh, L.-H. Lu, L. P. B. Katehi, P. Bhattacharya, E. T. Croke, G. E. Ponchak and S. A. Alterovitz, "X- and Ku-band amplifiers based on Si/SiGe HBT's and micromachined lumped components," *IEEE Trans. Microwave Theory Tech.*,. vol. 46, pp. 685-694, May 1998.